Multifractal analysis of a semi-distributed urban hydrological model

Journal:	*Urban Water*
Manuscript ID:	NURW-2011-0130.R2
Manuscript Type:	Full Paper
Date Submitted by the Author:	n/a
Complete List of Authors:	Gires, Auguste; U. Paris-Est, Ecole des Ponts ParisTech, LEESU, Tchiguirinskaia, Ioulia; U. Paris-Est, Ecole des Ponts ParisTech, LEESU, Schertzer, Daniel; U. Paris-Est, Ecole des Ponts ParisTech, LEESU, Lovejoy, Shaun; McGill U., Physics dept
Keywords:	Data uncertainty, Rainfall-runoff analysis;, Hydroinformatics, Hydraulic of sewers, Modelling, Precipitation

Title: Multifractal analysis of a semi-distributed~~n~~ urban hydrological model ~~on a Seine-Saint-Denis study case~~

Authors:
A. Gires[1], I. Tchiguirinskaia[1], D. Schertzer[1], S. Lovejoy [2]

(1) U. Paris-Est, Ecole des Ponts ParisTech, LEESU, Marne-la-Vallee, France (auguste.gires@leesu.enpc.fr),
(2) McGill U., Physics dept., Montreal, PQ, Canada

Abstract:

The aim of this paper is to quantify the sensitivity of an operational semi-distributed urban hydrological/hydraulic model to rainfall variability. A 3 400 ha urban area located in Seine-Saint-Denis (North-East of Paris, France), is used as a case study. F~~In the f~~irst ~~part~~, spatio-temporal multifractal downscaling techniques are implemented on the C-band radar data (whose resolution is 1 km in space and 5 min in time) of the 9th February 2009 rainfall event to quantify the uncertainty associated with small scale unmeasured rainfall variability. It appears that the variability should not be neglected. This finding highlights the need to implement X-band radars (whose resolution is hectometric) in urban areas. Then, ~~In a second part~~ multifractal tools are used on both rainfall and simulated discharges that also exhibit a scaling behaviour. It appears that the rainfall drainage system basically transmits the rainfall variability without damping it, at least in terms of multifractal statistics.

Key words:
Rainfall variability, urban hydrology, multifractals, spatio-temporal downscaling

1) Introduction

Over the last decades, real time control (RTC) of urban drainage systems has experienced a fast development (see Schütze et al., 2004 for a review). Its traditional aim was to limit urban flooding and overflow. In the context of stronger regulations such as the Water Framework Directive (Council of European Communities, 2000), RTC is more and more dedicated to reducing urban pollution. This implies for instance limiting combined sewer overflows, which are a major source of river pollution (Pléau et al., 2005), or controlling discharge to optimize the efficiency of treatment plants (Schütze et al., 2004). In order to achieve these objectives RTC processes usually involve the use of urban hydrologic-hydraulic models.

The aim of this paper is to use the multifractal framework to test the sensitivity of such models to the spatio-temporal variability of the rainfall input. Universal multifractals (UM), which rely on concept of multiplicative cascades, are a standard statistical tool to analyze and simulate geophysical processes extremely variable over a wide range of scales with the help of a reduced number of parameters (see Lovejoy and Schertzer, 2007 for a recent review; Schertzer and Lovejoy, 1987, 1997). Such tools have been implemented on both rainfall and river discharge data. The comparison of their characteristic parameters (Tessier et al, 1996; Pandey et al., 1998; Labat et al., 2002; Tchiguirinskaia et al., 2007) and the behaviour of their extremes (Schertzer et al., 2006) have enabled to improve the understanding of the

rainfall/runoff relationship. To our knowledge these tools have not been implemented in the specific context of urban hydrology, where the impact of rainfall variability on discharge is enhanced. Indeed urban catchments are smaller with shorter response time, and the coefficients of imperviousness are greater leading to a greater proportion of quickly effective rainfall (Aronica and Cannarozzo, 2000; Segond et al., 2007).

In this paper we use an operational urban rainfall/runoff model that was calibrated on a 3,400 ha dominantly urban catchment, located in the county of Seine-Saint-Denis (North-East of Paris, France). With the use of radar rainfall estimate, this county has been implementing real time control of sewer networks since 1986 (Andrieux and Jacquet. 1987, Browne et al. 1998) to reduce overflow and pollution problems. The rainfall event of February 9th, 2009 is analyzed in this paper.

The paper is organized as follows. First the multifractal methodology is briefly presented (section 2). Then the rainfall event and the operational urban rainfall/runoff model are presented (section 3). The uncertainties associated with small scales rainfall variability are analysed in section 4. A focus on the variability occurring at scales smaller than 1 km x 1 km x 5 min, which is the usual resolution available with standard C-band radar networks, is made. Finally multifractal analysis on both rainfall and simulated discharges are performed to analyse whether the model reproduces or not the observed rainfall variability (section 5).

2) Multifractal methodology

The multifractal framework is presented with the help of rainfall fields, but it can be used to study or simulate any other geophysical field that is extremely variable over wide range of scales. The rainfall support, i.e. the portion of the field where it rains, can be characterized with the help of a fractal dimension d_F (Hubert and Carbonnel, 1988; Olson et al., 1993). Indeed the number of boxes N_λ needed to cover the rainfall support at a resolution λ ($=L/l$, the ratio between the outer scale L and the observation scale l) scales like:

$$N_\lambda \propto \lambda^{d_F} \quad (1)$$

The fractal co-dimension c_F is defined as the difference (d-d_F) where d is the dimension of the embedding space (d=1 for time series and d=2 for maps). It appears that this fractal dimension decreases when the threshold defining the occurrence of rainfall increases (Lovejoy et al., 1987; Hubert et al., 1995). Thus a single fractal dimension is not enough to characterize rainfall process, and an infinite number of fractal dimensions are needed. In the framework of multifractals, one expects the field R_λ to behave as λ^γ where γ is called "singularity" and is a scale invariant notion. The statistical properties such as the probability of exceeding not a threshold but a singularity (Eq. 2) or a statistical moment of order q of the field R_λ (Eq. 3) are power-law related to the resolution (Schertzer and Lovejoy, 1987):

$$\Pr\left(R_\lambda \geq \lambda^\gamma\right) \approx \lambda^{-c(\gamma)} \quad (2)$$

$$< {R_\lambda}^q > \approx \lambda^{K(q)} \quad (3)$$

Where $c(\gamma)$ and $K(q)$ are respectively the co-dimension function and the moment scaling function. These functions are related by the Legendre transform, and fully characterize the scaling variability of the studied process. When $c(\gamma)<d$, $c(\gamma)$ can be interpreted as the fractal co-dimension of the support of the field where it exceeds λ^γ.

For conservative Universal Multifractals (UM) (Schertzer and Lovejoy, 1987, 1997), $K(q)$ is characterized with the help of only 2 parameters:
- C_1, the mean intermittency co-dimension, which measures the clustering (intermittency) of the (average) intensity at smaller and smaller scales (C_1=0 for a homogeneous field);
- α, the multifractality index ($0 \le \alpha \le 2$), which measures the clustering variability with respect to intensity level.
The functions $c(\gamma)$ and $K(q)$ are then given by:

$$c(\gamma) = \frac{C_1}{\alpha - 1}\left(\frac{\gamma}{C_1 \alpha'} + \frac{1}{\alpha} \right)^{\alpha'} \qquad (4)$$

$$K(q) = \frac{C_1}{\alpha - 1}\left(q^{\alpha} - q \right) \qquad (5)$$

where $1/\alpha' + 1/\alpha = 1$. The DTM technique (Lavallée et al., 1993) was used to estimate the UM parameters.

In this paper, discrete multiplicative cascades are implemented to simulate UM (Pecknold et al., 1993). To achieve this, at each step of the cascade process, a structure such as a time step (in 1D) or a pixel (in 2D) is divided into λ_0 steps (in 1D) or λ_0^2 (in 2D) pixels respectively. The scale ratio $\lambda_0 = 2$ is commonly used, although this is not mandatory. The value affected to the sub-structure is the one of the parent structure multiplied by a random factor, chosen so that Eq. 3 and 5 remain valid. As a consequence, after n steps (the resolution of the cascade is $\lambda = \lambda_0^n$) the value of a given structure is the product of the random factors of the n previous steps of the cascade. Space and time can be considered at once in a cascade process. In the simplest space-time model (Marsan et al., 1996; Deidda, 2000; Biaou et al., 2003; Gires et al, 2011a, 2012a), when the spatial resolution is divided by λ_x, then the temporal one is divided by $\lambda_t = \lambda_x^{H_t}$, where H_t is the scaling anisotropy exponent between space and time (with H_t=1/3 for the rainfall). Thus a common choice is $\lambda_x = 3$ and $\lambda_t = 2$ ($3^{1-1/3} \approx 2.08$), which means that a structure is divided into 18 sub-structures at each step.

3) The case study

3.1) 9th February 2009 rainfall event

The rainfall event analyzed in this paper occurred in the Paris area on February 9th, 2009. The data comes from the C-band radar of Trappes operated by Météo-France, and located west of Paris at about 45 km from the studied catchment. The Météo-France processing includes correction of ground clutter, partial beam blocking and vertical profile of reflectivity effects (Tabary, 2007; Tabary et al., 2007). The resolution of the rainfall estimates is 1 km in space and 5 min in time. A square area of size 256 by 256 km centred on the radar during about 13 hours is analyzed. Figure 1 displays the estimated total rainfall depth (in mm) observed during this event. Characteristic radial features are visible and the results might be sensitive to them. Nevertheless the studied catchment (black box on Fig. 1), being close to the radar, should not be too affected. The use of dense X-band radar network could help overcome these difficulties, but such data are not available at the moment.

The validity of the multifractal framework is verified by displaying the statistical moments vs. the resolution for the rainfall data (see Eq. 3) in a log-log plot (Fig. 2a). The scaling behaviour is good over two distinct ranges of scales: 1-16 km (the coefficient of determination R^2 of the straight lines is equal to 0.96 on average) and 16-256 km (average R^2 equal to 0.97). Such scaling break was observed for other rainfall events in the Paris area (Tchiguirinskaia et al., 2011) or for a heavy rainfall event that occurred in the South of France on September 5-9th, 2005 (Gires et al., 2011a). The DTM technique (Lavallée et al., 1993) was implemented to estimate the UM parameters. C_1 and α were found to be equal respectively to 0.28 and 1.08 for large scales, and 0.056 and 1.52 for small scales. The empirical and theoretical (Eq. 5, with the estimated UM parameters) moment scaling functions $K(q)$ are plotted in Fig. 2b. The theoretical fitting is very good, except for small moments where the presence of numerous zeros generates a multifractal phase transition that biases the empirical estimate of $K(q)$. This behaviour is well retrieved by simply implementing a threshold on a simulated multifractal field (see Gires et al., 2012b for more details). Let us mention that these small moments are not used in the DTM technique, so that in that case the UM parameters estimates are not significantly affected, especially for the small scales, which are used in the downscaling technique.

3.2) The urban hydrologic/hydraulic urban model

The studied catchment is a predominantly urban area of approximately 3,400 ha located in the French county of Seine-Saint-Denis (North-East of Paris). The calibrated hydrologic/hydraulic model of the area (displayed in Fig. 3) was provided by the "Direction Eau et Assainissement de Seine-Saint-Denis" (the local authority in charge of urban drainage in this area). It is used operationally. The outlet is located in the West of the area. The semi-distributed model Canoe (Allison, 2005) was calibrated on this area. The catchment is divided into 198 sub-catchments which are considered as homogenous. Their size ranges from 0.9 to 92 ha, except for two of size 347 and 404 ha. The average size is 17 ha. The mean coefficient of imperviousness is 41%, with values ranging from 0 to 95%. The rainfall / runoff model for a sub-catchment is a linear reservoir. The major sewers are modelled leading to 69 km of links. Water flow in links is represented with the help of Saint-Venant equations. A basic feature of this area is its flatness. Indeed the mean slope of the links is about 0.009 m/m. The total rainfall depth during the event ranges from 19 mm in the North-West corner to 9 mm in the South East corner.

The modelled network exhibits a scaling behaviour and a fractal dimension can be computed with the help of the box counting method. To achieve this, a grid of pixels of size 20 m x 20 m was generated, and the pixels intersecting a link are considered to represent the network. A matrix of size 256 x 256 is then extracted (Fig. 4a) and the fractal dimension d_F is computed with the help of Eq. 1 (Fig. 4b displays this equation in a log-log plot). The scaling behaviour is good on two distinct ranges of scales separated by a break. Indeed the coefficients of determination of the straight lines, whose slopes are the fractal dimensions d_F, are equal to 0.994 and 0.999 for respectively small and large scales. For scales ranging from 20 to 160 m, d_F is equal to 1.09 which is quite close to 1. It implies that over small scales the fractal dimension describes only the linear structure of individual pipes and the not the structure of the whole sewer system. The size of 20 m x 20 m of the pixels of the original grid is likely to be too small with regards to the resolution of the modelled sewer network. For scales ranging from 160 m to 5 km, d_F is found to be equal to 1.68. The pluvial drainage network of the Val-de-Marne County (South-East of Paris) exhibits a similar behaviour with a fractal dimension

equal to 1.67 for scales ranging from 290 m to 18 km (Sarkis, 2008). Such scaling behaviour is also observed on natural river networks but with different characteristic parameter d_F . For instance Takayasu (1990) implemented the box counting technique on the Amazon and Nile Rivers and found fractal dimensions equal to respectively 1.85 and 1.4.

4) Quantifying the uncertainty associated with small scale rainfall variability

The aim of this section is to use the multifractal properties of rainfall to assess the uncertainty on sewer discharge associated with small scale rainfall variability, especially the one occurring at scales smaller than the C-band radar resolution (1 km^2 x 5 min), which is commonly provided by national meteorological services. More precisely the sensitivity of the semi-distributed urban hydrological/hydraulic model to rainfall resolution is tested. Assuming that the model properly represents the rainfall/runoff relation, it corresponds to the investigated uncertainty. The methodology implemented here is based on Gires et al. (2011b, 2012a). It basically consists in:

(i) Generating an ensemble of 100 realistic samples of stochastically downscaled rainfall field. The downscaling is achieved by stochastically continuing the space-time cascade process that was established over the available range of scales (section 3.1). Discrete cascades are implemented, with the UM parameters found for the small scales. The final resolution of the field is 111 m x 111 m x 1.25 min.

(ii) Simulating the corresponding ensemble of hydrographs with the help of the calibrated hydrological/hydraulic model (section 3.2). It should be mentioned that for technical reasons the temporal resolution is nevertheless degraded to the original 5 min.

The variability among these ensembles, which reflects the uncertainty associated with small scale rainfall variability, is then analyzed.

Two types of rainfall fields are used as initial input for the downscaling process. The first case corresponds to the raw radar estimates whose resolution is 1 km x 1 km x 5 min. For the second case the same radar field was up-scaled (in space and time) to the resolution of 9 km x 9 km x 20 min. As a consequence, 2 steps of space-time cascades are implemented in the first case, and 4 steps are implemented in the second one. Figure 5 illustrates the downscaling of the rainfall field for both cases for an arbitrary time step. The same colour palette was used for the radar and downscaled fields to facilitate the comparison between the two. The variability created inside each radar pixel is clearly visible. The radar rainfall pixels are visible, and the discrete downscaling preserves this pixelization. The use of a continuous cascade (e.g., Schertzer et al., 1987) would have smoothed the spatial structure of the rainfall. As it can be seen on Fig. 5, in the second case a pixel of 9 km x 9 km almost covers the studied catchment, which means that the rainfall could be basically considered as uniform (in space). It should be mentioned that the downscaling technique ensures conservation on average. Indeed in the first case the average rainfall depth is equal to 15.1± 0.01 mm according to the sample and in the second case it is equal to 15.1± 0.2 mm. This means that the observed variability does not come from differences in the total rainfall amounts but from the differences in space-time rainfall distribution. The results of the first case are then compared with the ones of a similar study performed on a 900 ha urban area in Cranbrook in the North of London (see Gires et al., 2012a for more details). The rainfall event analysed in this case study occurred on the same day of February 9th, 2009. The data used are the Nimrod radar mosaics, a product of United-Kingdom Met Office.

Figure 6a displays the ensemble of hydrographs for both cases (in red for the first case and in black for the second case) for link 87 which is located in the West of the catchment. It appears that although exhibiting a similar overall pattern, the details of the curves are different. To clarify the disparities among these details, which are due to the uncertainty associated with small-scale rainfall variability, the 10 and 90% quantiles were evaluated for each time step. For both cases, the obtained curves (denoted respectively $Q_{0.1}$ and $Q_{0.9}$), are plotted with Q_{radar} (the flow simulated with the radar data at resolution 1 km x 1 km x 5 min and 9 km x 9 km x 20 min as rainfall input for the first and second cases respectively) in Fig. 6b. This figure provides a visual insight into the uncertainty, which is visible on the whole hydrograph and tends to increase with flow. As expected the curves for the first case are embedded in the ones of the second case, which reflects the fact that the uncertainty is greater for the reduced initial rainfall resolution (i.e. with 9 km x 9 km x 20 min grid size).

A more quantitative approach is implemented for the peak flow for both cases. First the time of occurrence $t_{PF,radar}$ of the peak flow with the radar rainfall input is retrieved. Then for each simulation the flow at $t_{PF,radar}$ is evaluated, and the corresponding histogram is plotted. This is illustrated in Fig. 6c and 6d for respectively the first and second cases, and with the same scale, so that they can be compared. As expected the histogram is much wider in the second case. The variability among the ensemble is quantified with the help of a pseudo coefficient of variation, defined as:

$$CV'_{(1)} = \frac{Q_{0.9}(t_{PF,radar}) - Q_{0.1}(t_{PF,radar})}{2 * PF_{radar}} \quad (6)$$

The corresponding indicator for the second case ($CV'_{(2)}$) is also evaluated. *CV'* characterizes the middle portion of the histogram. A greater *CV'* corresponds to greater variability among the ensemble of peak flows and therefore to stronger uncertainty.

A map of the coefficient $CV'_{(1)}$ is shown in Fig. 7. It appears that as expected *CV'* tends to decrease with downstream links, which reflects the fact that the uncertainty associated with small scale unmeasured rainfall variability becomes smaller with greater drained area. *CV'* is almost negligible for the outlet and reaches approximately 25 % for many upstream links. It should be noted that relatively great values are found for upstream links despite the coarse resolution of the model (the square root of the average catchment area is 412 m) with respect to the resolution of the downscaled rainfall field (111 m), which in itself does not enable to fully represent rainfall variability. These results are similar to the ones obtained on the London case study where *CV'* was equal to 3.4% for the outlet (the size of the studied area is roughly four times smaller than the one of the Paris case study) and reached 20% for upstream conduits, with an increase in between according the area drained by the conduit (see Fig. 10 of Gires et al., 2012a for a visual illustration). Concerning $CV'_{(2)}$ a map exhibiting a similar pattern, but with greater values, is obtained. To clarify this point Fig. 8 displays $CV'_{(1)}$ and $CV'_{(2)}$ in a scatter plot. Although no clear tendency is visible on the graph, it appears that $CV'_{(2)}$ is more than twice greater than $CV'_{(1)}$. Figure 8 enables to quantify the improvement provided by the use of a C-band radar whose resolution is 1 km x 1 km x 5 min rather than an almost uniform rainfall over the catchment. It is interesting to note that the values of *CV'* found are of the same order of magnitude as the relative error (in absolute value) made on the peak flow by inputting the radar rainfall at a resolution of 9 km x 9 km x 20 min rather than the available one of 1 km x 1 km x 5 min. Indeed this relative error is greater than 10% and 20% for more than respectively a third and a tenth of the modelled links. The use of X-band radar whose spatial resolution is about 100 m would enable to limit the uncertainty assessed with $CV'_{(1)}$. This shows that the uncertainty associated with small scale rainfall variability

cannot be neglected and should therefore be taken into account in real time management of storm water sewer networks.

Although the aim of this section was to test the sensitivity of the model to rainfall resolution, its validity was also verified. To achieve that, the water level measurement by a gauge located in the storage basin 1 (see Fig. 9b for a scheme of the local configuration) is compared with the water level simulated in the large link that represents it (Fig. 9c). The water reaching this link comes from a 256 ha area, which is divided into 4 sub-catchments in the model (Fig. 9a). It should be mentioned that these sub-catchments are among the greatest, which may affect the reliability of the simulated flow. As it can be seen on Fig 9b, the filling of the basins strongly depends on the management of the two gates. Figure 9d shows the temporal evolution of the measured water level. Two ways of managing the gates are tested: the standard one (this is the one usually used in this study, in blue on Fig. 9d), and the one that was actually implemented during this event (in red on Fig 9d). The overall behaviour is quite similar. The differences are mainly visible in the timing of the beginning of the water level increase and of the opening of gate 1 that triggers the sharp decrease in water level at the end of the simulation. These events are more realistically reproduced when the actual management of the gates is implemented. In the following of this section, we will only discuss this case. The increase of water level is rather well represented by the model. Nevertheless, after 5.5h of simulation the model simulates first a decreasing and then steady water level, whereas the measurements indicate an increasing one, although increasing slower than during the period of first 5.5h. This is likely to be due to the differences between the actual configuration of the basins (Fig. 9b) and its representation in the model (Fig. 9c), which does not enable to accurately simulate flow. Indeed the two basins are modelled by two large pipes, and furthermore in the model gate 2 does not link the second basin directly to the first one, but to the node PMB0. As a consequence when gate 2 is opened in the model (as it is the case after 5.5h in our case) the water is not released to the first basin, and instead goes directly to the node PMB0. Thus the water level does not increase in the first basin as it was measured. The impact of the small scale rainfall variability (starting with a rainfall resolution of 1km*1km*5min) is illustrated with the help of the curves in dashed red in Fig. 9d, which represent the 10 and 90% quantiles for each time step in the ensemble of simulated hydrographs (see previously in the section for more details about the methodology). This uncertainty is basically visible only during the period with the highest water levels. It should be noted that the rather great size of these sub-catchments does not enable to fully take advantage of the rainfall downscaling.

5) Retrieving the rainfall multifractal behaviour on discharges

The aim of this section is to use the multifractal tools to analyse the output of the studied hydrological/hydraulic urban model. A preliminary analysis was performed on hydrographs simulated with the 9th February 2009 rainfall event (see previous section). As suggested by Tessier et al. (1996) the analysis is done not directly on the discharge, but on the fluctuations of the discharge. Indeed the multifractal techniques that are implemented here assume that the studied field is conservative. Non-conservative field are represented as a conservative one (characterized by C_1 and α) multiplied by non-conservative part characterized with the help of an additional parameter H. In order to retrieve robust estimates of the UM parameters C_1 and α of non conservative fields (such as discharge time series) one has to perform the analysis on

the underlying conservative field which is commonly approximated by the absolute value of the fluctuation (for each time step, the value is replaced by the absolute value of the difference between this value and the one of the next time step) (Lavallée et al., 1993). The analysis is done on 128 time steps of 5 min (roughly 11 h). It appears that although limited in range of scales, a scaling behaviour is visible for all the links. There is no clear tendency for the scale at which the break occurs according to the position of the link in the network (either upstream or downstream). It seems that there are basically no differences in the scaling behaviour between the hydrographs simulated with the help of the raw rainfall field or the downscaled one. Given the very low amount of data (i.e., a sample of 128 time step values), these results may not be very reliable. They only give an indication that the model seems to simulate hydrographs exhibiting a scaling behaviour. To confirm this and to investigate the consequences, the following methodology was implemented:
(i) Generation of 100 high resolution (111 m x 111 m x 1 min) realistic rainfall events lasting 256 min and exhibiting a scaling behaviour.
(ii) Simulation of the corresponding hydrographs with the help of the calibrated hydrological/hydraulic model (see section 3.2)
(iii) Performing a multifractal analysis on the ensemble of 100 hydrographs. Each hydrograph is considered as a realisation of the same phenomenon, up-scaled independently and then taken into account in Eq. 3, which theoretically is valid for an ensemble average, with a large number of realisations.

The rainfall fields are generated with the help of space time discrete UM cascades. The UM parameters used are those estimated for the small scales of the studied rainfall event (α=1.52, C_1=0.056) without any break. Indeed the outer scale of the studied catchment is 12 km, which is smaller than the scale at which the break occurs for the rainfall field (16 km). The final resolution of the simulated field is 111 m x 111 m x 1 min, and the event lasts 256 min. The fields are renormalized so that the mean total rainfall depth over the studied area is the same for all the events and corresponds roughly to a 5 years return period event. As suggested by "l'Instruction Technique de 1977" (1977), which is a technical document issued by the French government and describing the rules that should be implemented to design a sewer system, the Montana Formula was used:

$$I(D,T) = a(T)D^{b(T)} \quad (7)$$

where D (min) is the duration of the rainfall event, T (year) is the return period, and I (mm/min) is the intensity. For the Paris area, a = 5 and b = -0.61 for a 5 year return period. This leads to a mean rainfall rate of 10.2 mm/h that corresponds to a total rainfall depth of 43.5 mm during the entire event. There is no need to correct this value for such size of studied area (9 km x 12 km) and duration (256 min). Indeed the ratio between the average rainfall over the area and the point rainfall given by the Montana formula would be greater than 0.95 (Roux, 1996). Anyway taking it into account would simply mean that the total rainfall depth considered corresponds to a rainfall event of return period slightly greater than 5 years.

Before discussing the UM parameters estimates, it is necessary to assess the quality of the scaling behaviour. For some links, scaling is not observed on the whole range of scales (1min – 256 min). Indeed a break is visible at scales ranging from 2 to 16 min according to the link. As a consequence, an automatic algorithm was developed to determine the scale at which the break occurs: (i) The scaling curve (i.e. Eq. 3 in a log-log plot) is plotted
(ii) The mean coefficient of determination (R^2) for large scales (i.e. the left part of the graph) is evaluated when a break is considered at 1, 2, 4, 8, and 16 min.
(iii) At the beginning no break is considered. Then if R^2(break at 2 min) – R^2 (break at 1 min)< 0.04, then no break is considered. Otherwise a break is considered at 2 min and the

process is iterated with R^2(break at 4 min) to check whether it should be at 4 min. And so on if needed up to 16 min. This process enables to take into account the largest relevant range of scales.

A good scaling behaviour is retrieved for large scales (the mean R^2 is equal to 0.98). An illustration for link 87 is given in Fig. 10. In the following the small scales are not taken into account because their behaviour would be assessed with the help of a too low number of points, and furthermore for links where there are 3 or more points the average R^2 is equal to 0.95 which is quite low. Figure 11a displays a map with the scale at which the break occurs for all the links. The characteristic scale of the break tends to be larger with downstream links. Basically no break is observed for upstream links. Near the outlet, the separation of the flow in two parallel links breaks the scaling behaviour, which is retrieved downstream. Overall the discharges simulated with the model basically do not reproduce the rainfall scaling behaviour for scales smaller than 5 min. This is likely to be due to the damping effect of the lumped model that is used for each sub-catchment.

The UM parameters were estimated for all the links. For most of the conduits α and C_1 belong respectively to the range 1.6-1.9 and 0.05-0.1. Figures 11b and 11c display maps of α and C_1. There is no clear tendency over the distribution of the values in the network. It is striking to note that both UM parameters used to simulate the rainfall fields (i.e. α=1.52 and C_1=0.056) seem to be smaller than the ones found for discharge. This single fact does not mean that the extremes are strengthened in the sewer network with regards to rainfall. Indeed the dimension of the embedding space which is different for the discharge time series and the space-time rainfall should be taken into account. To clarify this issue, let us consider the scale invariant notion of maximum probable singularity γ_s, which assesses the extremes (Hubert et al., 1993, Douglas and Barros, 2003, Royer et al., 2008, Gires et al., 2011a). It is defined as the maximum probable singularity observable on a unique sample of phenomenon. It corresponds to the singularity for which the fractal codimension of the support $c(\gamma_s)$ becomes equal to the dimension d of the embedding space. Here, d = 1 for the discharge time series, and d = 8/3 = 2+2/3 for the space-time simulated rainfall fields. $\gamma_{s,rainfall}$ is equal to 0.51 and Fig. 11d displays a map of γ_s for all the links. It appears that $\gamma_{s,rainfall}$ is comparable to γ_s for most of the links, may be with a tendency to be slightly greater. This means that the sewer network basically reproduces rainfall extremes and does not damp them or only slightly does.

6) Conclusion

The aim of the paper was to test, with the help of multifractal tools, the sensitivity of an operational urban rainfall/runoff model to the rainfall spatio-temporal variability. The study was conducted on a 3 400 ha urban area located in Seine-Saint-Denis, in the North of Paris (France). The rainfall event of February 9th, 2009 was used.

First a stochastic ensemble approach was implemented to quantify the uncertainty of discharge estimates, associated with the rainfall variability occurring at scales smaller than 1 km x 1 km x 5 min which are usually available with C-band radar networks. An analysis of the quantiles of the simulated peak flow showed that the uncertainty exceeds 20 % for upstream links. A similar analysis, but starting with a rainfall resolution of 9 km x 9 km x 20 min, showed a clear decrease in uncertainty when the C-band radar resolution is used. This analysis highlights the interest of implementing X-band radars in urban areas. Indeed such

radars provide data with a hectometric resolution that would enable a better management of storm water. Meanwhile the uncertainty associated with small scale unmeasured rainfall variability, which cannot be neglected, should be taken into account in a probabilistic way in the real time management of sewer systems. Further investigations should be carried out with other types of rainfall, especially more convective ones with more localized rain cells for which greater uncertainty is expected.

Second the multifractal properties of the simulated hydrographs were analysed with the help of simulated rainfall fields of resolution 111 m x 111 m x 1 min, lasting 4 hours, and corresponding to a 5 year return period event. On the whole, the discharges exhibit a good scaling behaviour on the range 4 h – 5 min. Both UM parameters tend to be greater for the discharge than for rainfall. The notion of maximum probable singularity was used to clarify the consequences on the assessment of extremes. It appears that the sewer network basically reproduces the extremes, or only slightly damps them, at least in terms of multifractal statistics.

This paper suggests a new way of testing hydrological models. Further investigations involving other models with greater spatial resolution and taking into account the interactions between surface and sewer flows (Maksimovic et al., 2009) and event sub-surface flows (El Tabbach et al., 2009) should be performed.

Acknowledgements

The authors acknowledge Météo-France for providing the radar rainfall estimates in an easily exploitable format, and especially Jacques Parent du Chatelet, Gilbert Gayraud and Catherine Hamet, and the "Direction Eau et Assainissement" of Seine-Saint-Denis for providing a calibrated hydrological-hydraulic model the studied area, and the help of the Julien Richard (LEESU) to obtain the Fig 3. The authors greatly acknowledge partial financial support form the Chair "Hydrology for Resilient Cities" (sponsored by Veolia) of Ecole des Ponts ParisTech, EU FP7 SMARTeST project (www.floodresilience.eu), and EU NWE Interreg IV RainRain project (www.raingain.eu).

References

Allison, INSA Lyon, SOGREAH Consultants, www.canoe-hydro.com (2005). Manuel d'utilisation de Canoe.

Andrieu, H. and Jacquet, G., 1987. Le radar météorologique de Trappes et l'estimation des intensités pluvieuses en Seine-Saint-Denis. Intérêt pour la gestion des réseaux d'assainissement. La Houille Blanche, 6 (Sept. 1987), 447-457.

Aronica, G. and Cannarozzo, M., 2000. Studying the hydrological response of urban catchments using a semi-distributed linear non-linear model. *J. Hydrol.*, 238, 35-43.

Biaou, A., Hubert, P., Schertzer, D., Tchiguirinskaia, I. and Bendjoudi, H., 2003. Fractals, multifractals et prévision des précipitations. *Sud Sciences et Technologies*, 10, 10-15.

Browne, O., Auriaux, G., Idier, F. and Delattre, J.M., 1998. Un système d'aide à la décision pour la conduite du réseau d'assainissement de Seine-Saint-Denis. *Novatech'98 Proceedings*, Lyon, May 4-6th 1998.

CEC—Council of the European Communities, 2000. Directive of establishing a framework for community action in the field of water policy. EC Directive No. 2000/60/EEC of 23 October 2000.

Deidda, R., 2000. Rainfall downscaling in a space-time multifractal framework. *Water Resour. Res*., 36, 1779-1794.

Douglas, E and Barros, A., 2003. Probable Maximum Precipitation Estimation using Multifractals : Application in the Esatern United States. *Journal of Hydrometeorology*, 4, 1012-1024.

El Tabach, E., Tchiguirinskaia, I., Mahmood, O. and Schertzer, D., 2009. Multi-Hydro: a spatially distributed numerical model to assess and manage runoff processes in peri-urban watersheds. Proceedings Final conference of the COST Action C22 Urban Flood Management, Paris 26/27.11.2009, France.

Gires, A., Tchiguirinskaia, I., Schertzer, D. and Lovejoy, S., 2011a. Analyses multifractales et spatio-temporelles des précipitations du modèle Méso-NH et des données radar. *Hydrol. Sci. J.,* 56 (3), 380-396.

Gires, A.., Schertzer, D., Tchiguirinskaia, I., and Lovejoy, S., Maksimovic, C., Onof, C. and Simoes, N., 2011b. Impact de la variabilité non-mesurée des precipitations en hydrologie urbaine: un cas d'étude dans le cadre multifractal. *La houille Blanche,* **4**, 37-42.

Gires, A.., Onof, C., Maksimovic, C., Schertzer, D., Tchiguirinskaia, I. and Simoes, N., 2012a. Quantifying the impact of small scale unmeasured rainfall variability on urban hydrology through multifractal downscaling: a case study. *J. Hydrol*., 442-443, 117-128.

Gires, A., Tchiguirinskaia, I., Schertzer, D., and Lovejoy, S., 2012b. Influence of the zero-rainfall on the assessment of the multifractal parameters. *Adv. Water Resour., In press* http://dx.doi.org/10.1016/j.advwatres.2012.03.026

Hubert, P. and Carbonnel, J.P., 1988. Caractérisation fractale de la variabilité et de l'anisotropie des précipitations tropicales. *C. R. Acad. Sci. Paris*, 2, 909-914.

Hubert, P., Tessier, Y., Lovejoy, S., Schertzer, D., Schmitt, F., Ladoy, P., Carbonnel, J.P. and Violette, S., 1993. Multifractals and extrem rainfall events. *Geophys. Lett.* ,20, 931-934.

Hubert, P., Friggit, F., Carbonnel, J.P., 1995. Multifractal structure of rainfall occurrence in west Africa. In: Z. W. Kundzewicz, ed. *New uncertainty concepts in hydrology and water resources.* Cambridge: Cambridge University Press, 109-113.

Instruction Technique, 1977. Instruction technique relative aux réseaux d'assainissement des agglomérations, Imprimerie nationale, juin 1977.

Labat, D., Mangin, A. and Ababou, R., 2002. Rainfall–runoff relations for karstic springs: multifractal analyses. *J. Hydrol*., 256, 176–195.

Lavallée, D., Lovejoy, S. & Ladoy, P., 1993. Nonlinear variability and landscape topography: analysis and simulation. In: L. De Cola and N. Lam, eds. *Fractals in geography*. New York: Prentice-Hall, 158-192.

Lovejoy, S., Schertzer, D., and Tsonis, A.A., 1987. Function box-counting and multiple elliptical dimension in rain. *Science*, **235**(4792), 1036-1038.

Lovejoy, S. and Schertzer, D., 2007. Scale, scaling and multifractals in geophysics: twenty years on. In: A.A. Tsonis & J. Elsner, eds. *Nonlinear dynamics in Geosciences.* Springer, 311-337.

Maksimović, Č., Prodanović, D., Boonya-aroonnet, S., Leitão, J. P., Djordjević, S. and Allitt, R., 2009. Overland flow and pathway analysis for modelling of urban pluvial flooding. *Journal of Hydraulic Research,* 47 (4), 512–523.

Marsan, D., Schertzer, D. and Lovejoy, S., 1996. Causal space-time multifractal processes: Predictability and forecasting of rain fields. *J. Geophys. Res.*, 101, 26,333-326,346.

Olsson, J., Niemczynowicz, J. and Berndtsson, R., 1993. Fractal analysis of high-resolution rainfall time series. *J. Geophys. Res.,* 98, 23265-23274.

Pecknold, S., Lovejoy, S., Schertzer, D., Hooge, C. and Malouin, J.F., 1993. The simulation of universal multifractals. *In*: J.M. Perdang and A. Lejeune, eds. *Cellular Automata: Prospects in astrophysical applications*. World Scientific, 228-267.

Pandey, G., Lovejoy, S. and Schertzer, D., 1998. Multifractal analysis including extremes of daily river flow series for basins one to a million square kilometres. *J. Hydrol*., 208 (1-2), 62–81.

Pléau, M., Colas, H., Lavallée, P., Pelletier, G. and Bonin, R., 2005. Global optimal real-time control of the Quebec urban drainage system. *Environmental Modelling & Software*, 20, 401-413.

Roux, C., 1996 Analyse des précipitations en hydrologie urbaine. Exemple de la Seine-Saint-Denis. PhD Thesis, Ecole des Ponts ParisTech, Marne-la-Vallée, France. p.290.

Royer, J.F., Biaou, A., Chauvin, F., Schertzer, D. and Lovejoy, S., 2008. Multifractal analysis of the evolution of simulated precipitation over France in a climate scenario. *C.R Geoscience 340,* 431-440.

Sarkis, B., 2008. *Etude multi-échelle des réseaux d'assainissement*. MSc Thesis. Ecole des Ponts ParisTech.

Schertzer, D. and Lovejoy, S., 1987. Physical modelling and analysis of rain and clouds by anisotropic scaling and multiplicative processes. *J. Geophys. Res.,* 92(D8), 9693-9714.

Schertzer, D., and Lovejoy, S., 1997. Universal multifractals do exists!: Comments. Journal of Applied Meteorology, 36(9), 1296-1303.

Schertzer, D., Bernardara, P., Biaou, A., Tchiguirinskaia, I., Lang, M., Sauquet, E., Bendjoudi, H., Hubert, P., Lovejoy, S. and Veysseire, J.M., 2006. Extrêmes et multifractals en hydrologie : résultats, validations et perspectives. *La Houille Blanche,* 5, 112-119.

Schütze, M., Campisano, A., Colas, H., Schilling, W. and Vanrollegheme, P.A., 2004. Real time control of urban wastewater systems—where do we stand today? *J. Hydrol*, 299, 335–348

Segond, M-L., Wheater, H.S. and Onof, C., 2007. The significance of small-scale spatial rainfall variability on runoff modeling. *J. Hydrol.*, 173, 309-326.

Tabary, P. (2007). The new French operational radar rainfall product. Part I: Methodology. *Wea. Forecasting*, 22, 393–408.

Tabary, P., Desplats, J., Do Khac, K., Eideliman, F., Gueguen, C., and Heinrich, J.-C., 2007. The new French operational radar rainfall product. Part II: Validation. *Wea. Forecasting*, 22, 409–427.

Takayasu, H., 1990. Fractals in the Physical Sciences. Manchester University Press, Manchester.

Tchinguirinskaia, I., Schertzer, D., Hoang, C.T. and Lovejoy, S., 2011. Multifractal study of three storms with different dynamics over the Paris region. Proceedings of Weather radar and hydrology symposium, Exeter, UK, April 2011.

Tchiguirinskaia, I., Schertzer, D., Hubert, P., Bendjoudi, H. and Lovejoy, S., 2007. Potential of multifractal modelling of ungauged basins. PUB Kick-Off Meeting. D. Schertzer et al. Wallingford, UK, IAHS Press. 309: 298-308.

Tessier, Y., Lovejoy, S., Hubert, P., Schertzer, D., Pecknold, S., 1996. Multifractal analysis and modeling of rainfall and river flows and scaling, causal transfer functions. *J. Geophys. Res.*, 101 (D21), 26,427-26,440.

Figure captions:

Figure 1. Map of the total rainfall depth (in mm) during the rainfall event of February 9th, 2009. The area is of size 256 by 256 Km, and the coordinate system is the "extended Lambert II" system (unit = hm). The Meteo-France C-band radar of Trappes is located in the centre of the image. The studied catchment is indicated by the black box.

Figure 2. (1) Illustration of the definition of the moment scaling function (Eq. 3) for the rainfall event of February 9th, 2009. (2) Empirical and theoretically fitted $K(q)$ functions for both small and larges scales.

Figure 3. The studied portion of the Seine-Saint-Denis county and the modelled underground sewer system (this figure was obtained with the help of Julien Richard).

Figure 4. (a) Representation of a portion of the modelled sewer network with the help of boxes of 20 m size. (b) Determination of the fractal dimension of the sewer network with the help of box counting method (Eq. 1)

Figure 5. Illustration of the space-time downscaled rainfall fields (from a resolution of 1 km^2 x 5 min, and from one of 9 km x 9 km x 20 min) over the studied area for an arbitrary time step.

Figure 6. All the graphs are for link 87. The red and black curves correspond to the first and second cases respectively. (a) 100 samples of simulated hydrographs. (b) Hydrographs $Q_{0.9}$ (dash), $Q_{0.1}$ (dash), and Q_{radar} (solid). (c) and (d) Histogram of the peak flow of the 100 samples.

Figure 7. Map of $CV'_{(1)}$ for all the modelled links.

Figure 8. Scatter plot of $CV'_{(1)}$ and $CV'_{(2)}$

Figure 9. (a) Snapshot of the Canoe model of the 4 sub-catchments whose water is drained toward the link with available water level measurements. (b) Actual configuration of the two basins, where water level measurements are available. (c) Representation of these basins in the Canoe model. (d) Temporal evolution of the water level in the studied link (which corresponds to the basin 1): measured (black), simulated with standard gate management (blue), simulated with actual gate management (solid red) and the corresponding uncertainty associated with small scale rainfall variability (dashed red).

Figure 10. Illustration of the scaling behaviour (i.e. Eq. X in a log-log plot) for the simulated discharge of link 87. Here the break occurs at 2 min.

Figure 11. Maps of the temporal scale of the scaling break (a), α (b), C_1 (c), and γ_s (d) for all the modelled links of the sewer system.

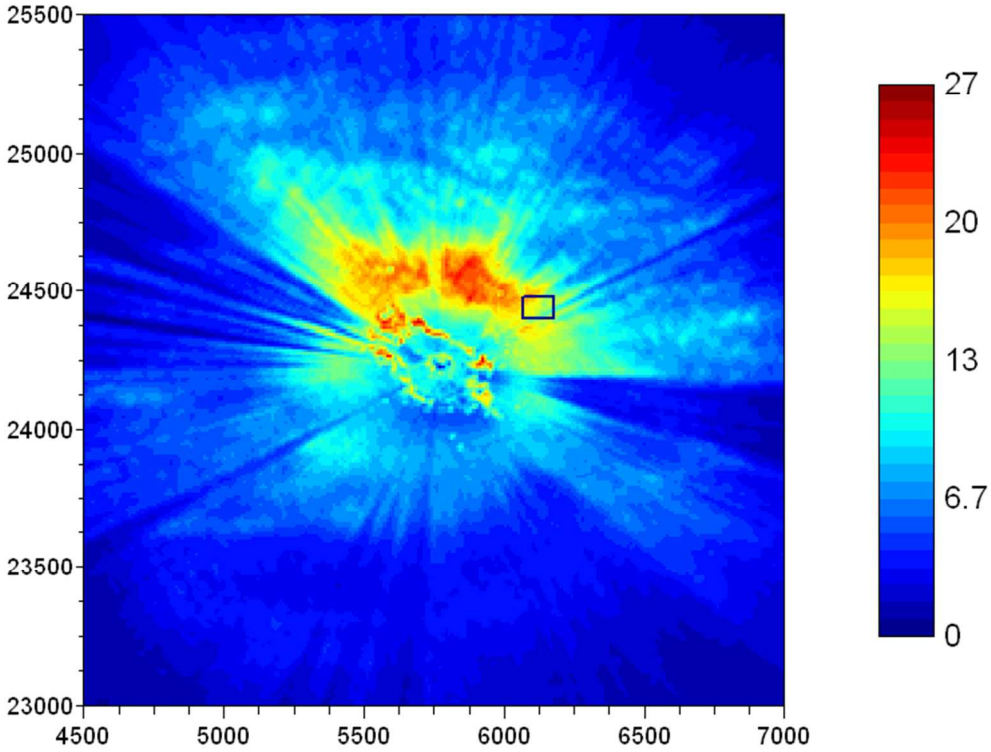

Figure 1. Map of the total rainfall depth (in mm) during the rainfall event of February 9th, 2009. The area is of size 256 Km, and the coordinate system is the "extended Lambert II" system (unit = hm). The Meteo-France C-band radar of Trappes is located in the centre of the image. The studied catchment is indicated by the black box.
198x150mm (96 x 96 DPI)

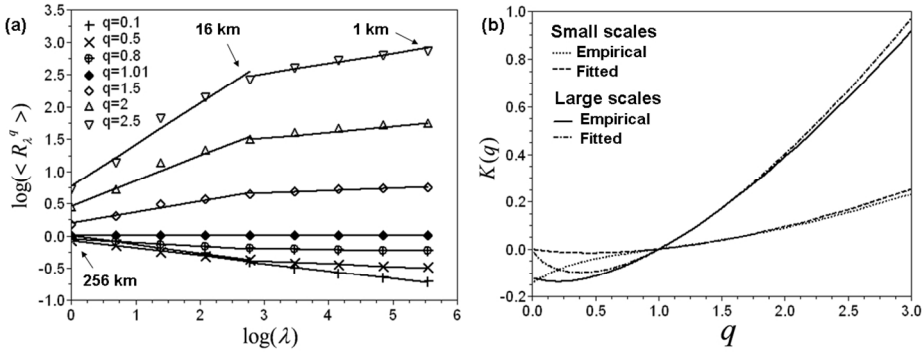

Figure 2. (1) Illustration of the definition of the scaling moment function (Eq. 3) for the rainfall event of February 9th, 2009. (2) Empirical and theoretically fitted K(q) functions for both small and larges scales. 356x135mm (96 x 96 DPI)

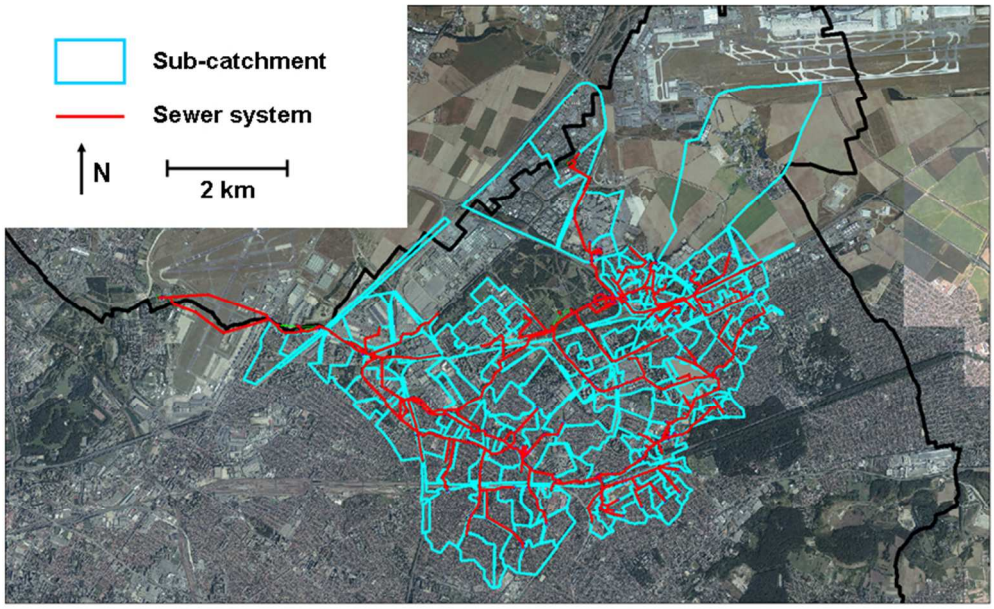

Figure 3. The studied portion of the Seine-Saint-Denis county and the modelled underground sewer system (this figure was obtained with the help of Julien Richard).
233x144mm (96 x 96 DPI)

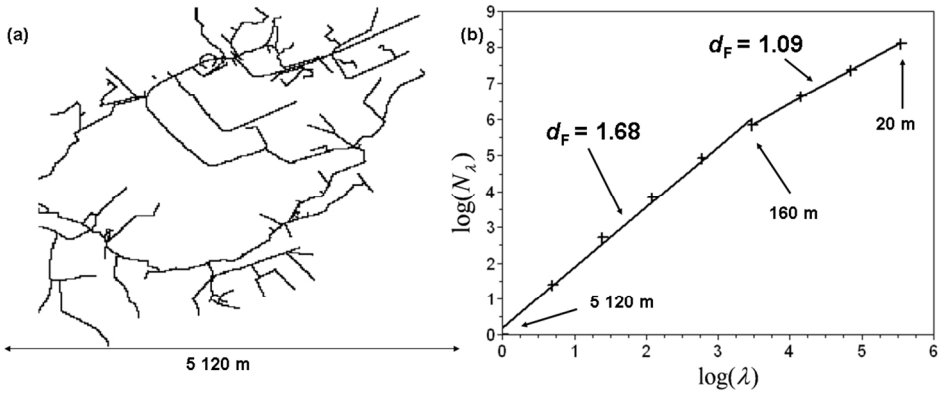

Figure 4. (a) Representation of a portion of the modelled sewer network with the help of boxes of 20 m size. (b) Determination of the fractal dimension of the sewer network with the help of box counting method (Eq. 1)
356x145mm (96 x 96 DPI)

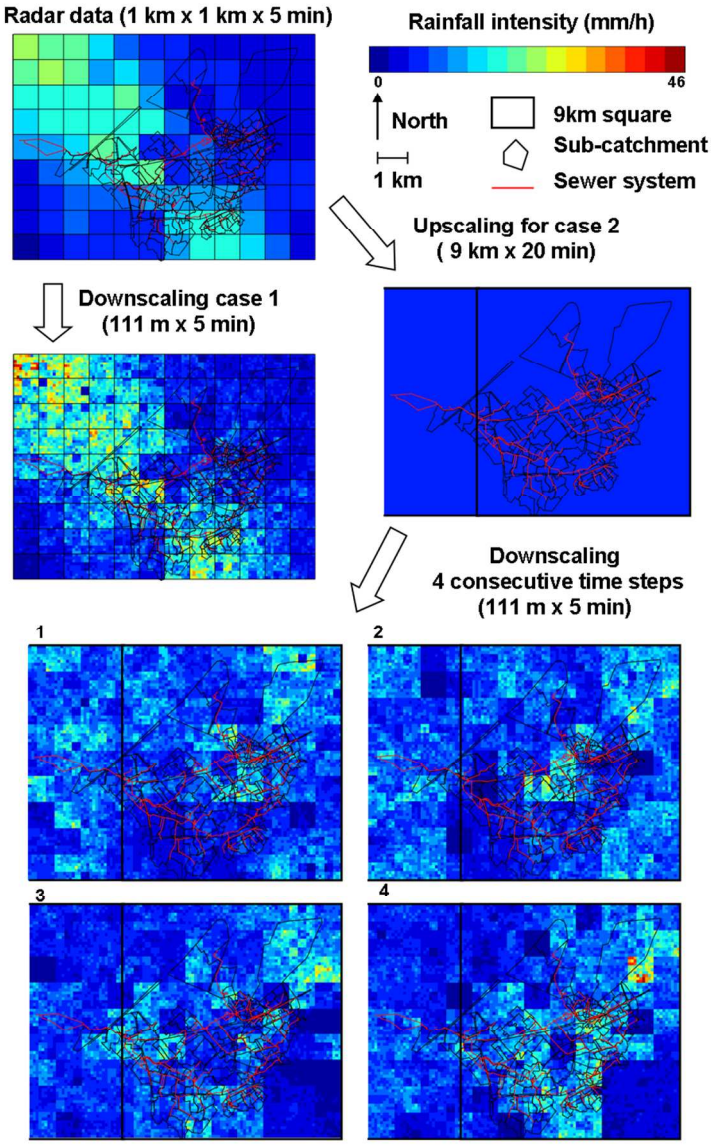

Figure 5. Illustration of the space-time downscaled rainfall fields (from a resolution of 1 km2 x 5 min, and from one of 9 km x 9 km x 20 min) over the studied area for an arbitrary time step.
250x400mm (96 x 96 DPI)

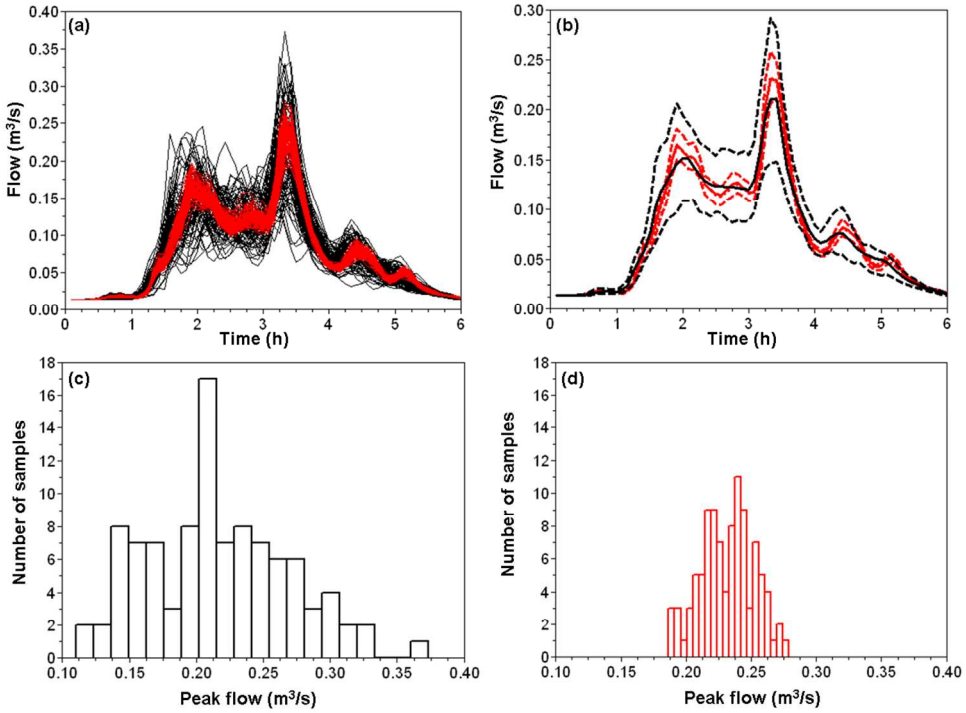

Figure 6. All the graphs are for link 87. The red and black curves correspond to the first and second cases respectively. (a) 100 samples of simulated hydrographs. (b) Hydrographs Q0.9 (dash), Q0.1 (dash), and Qradar (solid). (c) and (d) Histogram of the peak flow of the 100 samples.
356x261mm (96 x 96 DPI)

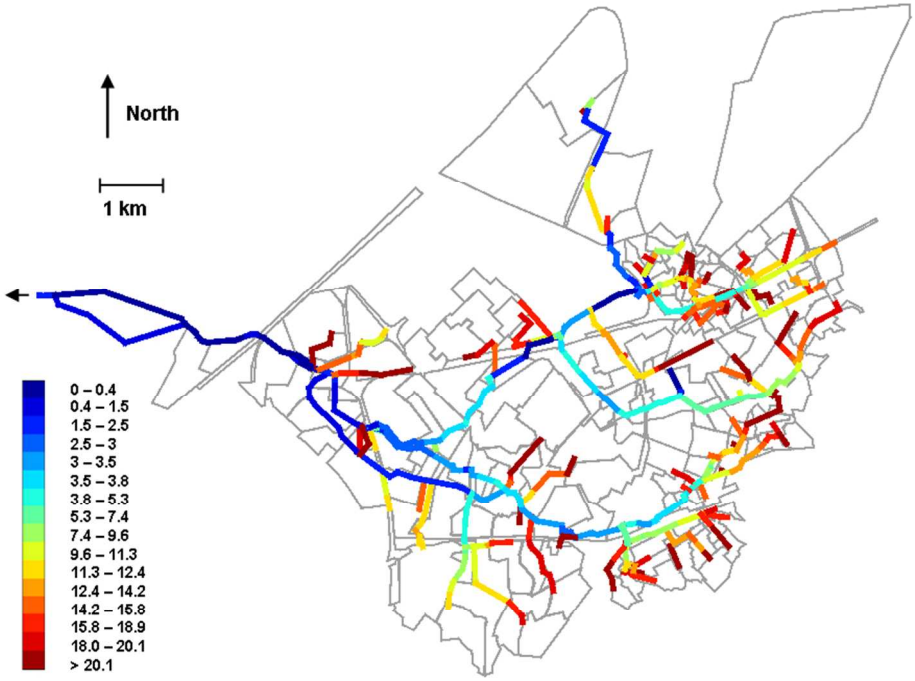

Figure 7. Map of CV'(1) for all the modelled links.
254x190mm (96 x 96 DPI)

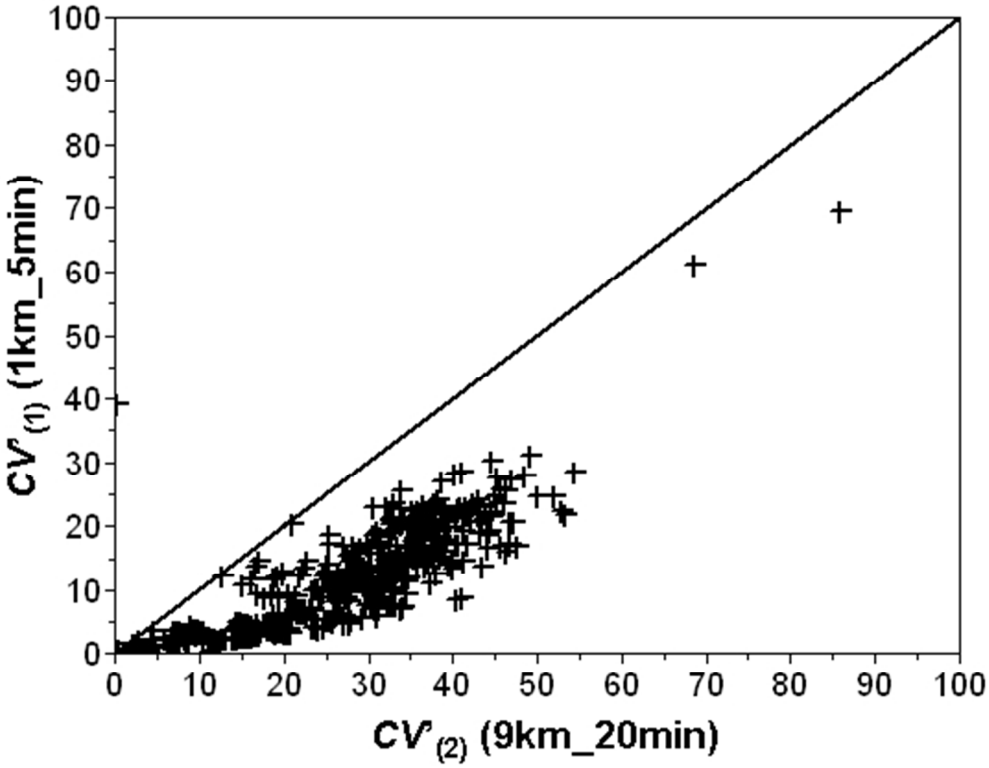

Figure 8. Scatter plot of CV'(1) and CV'(2)
143x112mm (96 x 96 DPI)

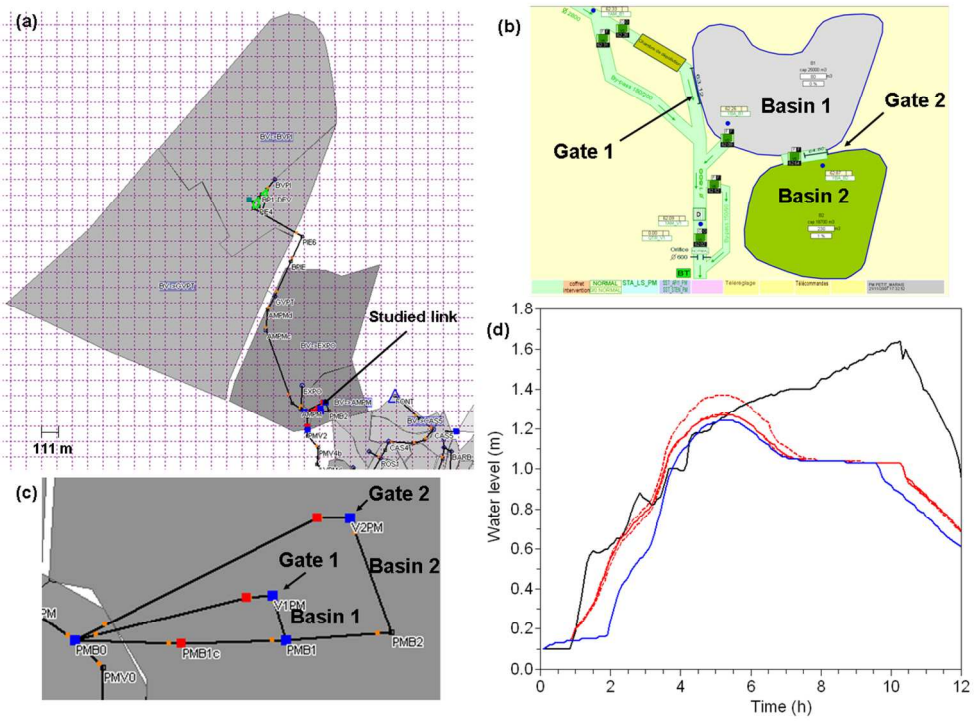

Figure 9. (a) Snapshot of the Canoe model of the 4 sub-catchments whose water is drained toward the link with available water level measurements. (b) Actual configuration of the two basins, where water level measurements are available. (c) Representation of these basins in the Canoe model. (d) Temporal evolution of the water level in the studied link (which corresponds to the basin 1): measured (black), simulated with standard gate management (blue), simulated with actual gate management (solid red) and the corresponding uncertainty associated with small scale rainfall variability (dashed red).
356x261mm (96 x 96 DPI)

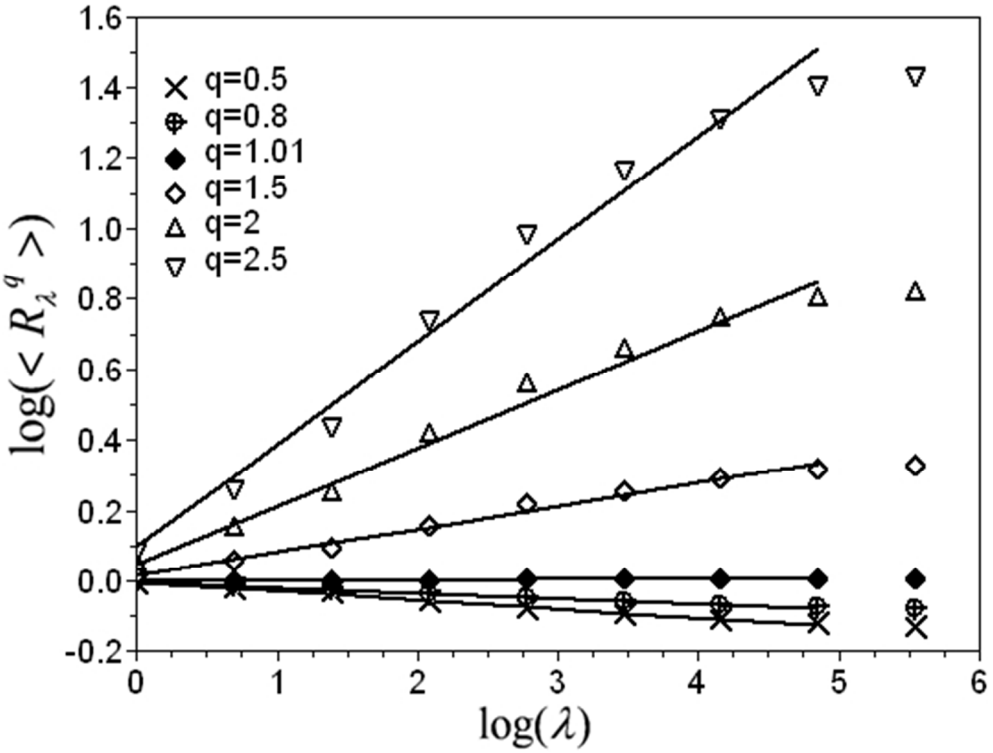

Figure 10. Illustration of the scaling behaviour (i.e. Eq. X in a log-log plot) for the simulated discharge of link 87. Here the break occurs at 2 min.
143x111mm (96 x 96 DPI)

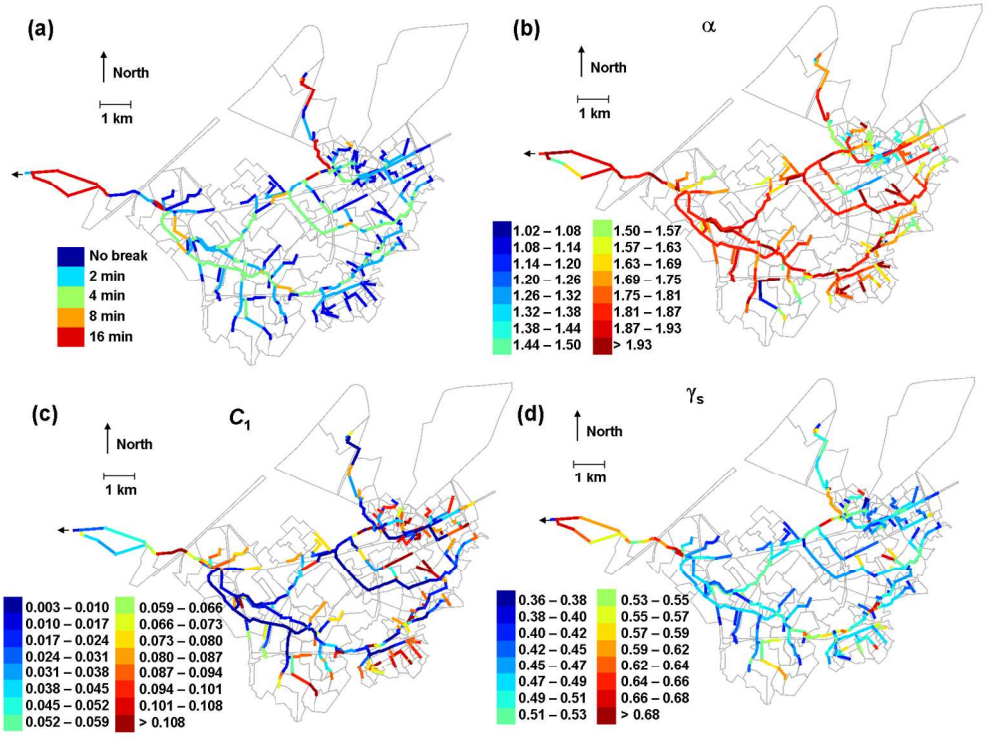

Figure 11. Maps of the temporal scale of the scaling break (a), α (b), C1 (c), and γs (d) for all the modelled links of the sewer system.
519x400mm (96 x 96 DPI)